

Trial of a Thermophotovoltaic Device in a Cement Cool Down Grate

Graham Buckley
Dublin Energy Laboratory
Technological University Dublin
Dublin, Republic of Ireland
graham.buckley@tudublin.ie

C. M. Iftekhar Hussain
Dublin Energy Laboratory
Technological University Dublin
Dublin, Republic of Ireland
cmiftekar.hussain@tudublin.ie

Brian Norton
Dublin Energy Laboratory
Technological University Dublin
Dublin, Republic of Ireland
brian.norton@tudublin.ie

Abstract— High temperature process industries reject up to 60 % of their thermal energy as waste heat that is difficult to recover due to high up-front costs and the complexity of installing conventional heat-recovery systems. Market research suggests that certain industries are willing to adopt Thermophotovoltaic (TPV) systems into their process as the technology becomes reliable and commercially viable. A Demonstration Model (DM) with 2 x GaSb cells was used to trial the technology in a laboratory and industrial context. The DM was exposed to a range of temperatures from 500 °C to 900 °C using an electric oven. The DM was tested in the cooldown grate of a cement factory where it produced 1.65 kW/m² at 1083 °C.

Keywords—*Thermophotovoltaic, Gallium-antimonide, Efficiency, Maximum-power-point, Industry Demonstration, Intensity*

I. INTRODUCTION

Thermophotovoltaics are a proven technology to convert infrared wavelengths of light into electricity by means of the photoelectric effect. The main advantages are scalability and diversity of shape and form with an energy density at a feasible efficiency. The disadvantages are a lack of heritage, obscurity, and high early-stage cost.

The development approach for this project is to use several de-risking models, the first of which is the Demonstration Model (DM). Two Gallium Antimonide (GaSb) cells are mounted to a water-cooled heat exchanger. This heat exchanger was made into a probe style device encased in high temperature borosilicate glass to protect the cells from direct exposure to dust and corrosive gasses. The DM was used to develop tools for analyses and to perform industrial trials.

Previous relevant research was focused on key TPV components such as; spectrally selective emitters, low band-gap cells, quantum dot shifting, parameters effecting performance from growing wafers, band-gap, multi junction cells, various theoretical models predicting performance, photonic crystals, etc. [1][2] [3][4]. However, few examples of full systems in industry settings were demonstrated. Some full-system examples include Coleman Lantern Si 1956 [5], GM Army Research Lab Ge generating 100W [6], JX Crystal GaSb 150W Midnight Sun [7], EDTEK Inc

GaSb 185W [8], Paul Scherrer Institute Si 50W [8], and MIT InGaAs 4.4W [9][10]. Previous laboratory experiments yielded promising results [11].

The objective of this research was to evaluate TPV system performance for industrial waste heat recovery application. The experiment measured the power density of GaSb cells and demonstrated their performance in a live factory setting. The electrical performances are detailed in this paper in terms of I-V curve, maximum power point (MPP), stability and drift, an estimation of efficiency and review of the experimental design.

II. EXPERIMENT METHOD

The results were gathered by exposing the DM to a cement cool down grate which complements prior laboratory work. The testing approach for the DM is one of gradually increasing strenuity, where the simpler testing occurred first. The MPP was studied with respect to temperature. The resistance between the anode and cathode of the cells was varied using a variable load driven by a microcontroller. With the measured voltage, the current was calculated by considering the variable load as a shunt resistor. Knowing circuit resistance and voltage allows for the calculation of an I-V curve.

An Arduino Uno R1 microcontroller with the ATMEGA 328P-PU was used. This was programmed using Arduino compiler 1.8.16. Libraries included were SPI.h, SD.h, RTClib.h, and max6675.h. External clock DS1307 and A MAX6657 was used for measuring temperature. Analysis was made using Python 3.8. Python optimization was made by the scipy.optimize package.

The resistance between the anode and cathode of the cells was varied from $\rightarrow 0 \Omega$ to $\approx 100 \Omega$. Voltage was measured across the shunt using the 10-bit ADC with a resolution of 0.0049V. The 8-bit pulse width modulation (PWM) output of the microcontroller was used to control the gate of a transistor. This simple setup has a higher resistance and time resolution with a tradeoff of higher noise level. The hookup wires connecting the TPV cells to the variable shunt resistor (VSR) had a total length of 12 m. This also contributed greatly to noise levels. An illustration of the electrical set-up is shown in Fig 1.

The setup can be automated, and multiple sweeps can be taken quickly. Since the Bit value of the PWM was known, the resistance of the circuit could be correlated by experimental calibration using a bench top power supply. Assuming the calibration is accurate, the voltage of the TPV cell can then be correlated to a resistance (varied by the PWM). Knowing the instantaneous resistance and voltage is necessary for the calculation of current across this part of the circuit. Ergo, the MPP can be measured automatically.

For these tests the DM used x2 GaSb TPV cells, together summing a surface area of 3 cm². One cell was orientated “up” (facing flat away from the ground) and “down” (facing flat towards the ground). Each cell produced ≈0.4 V at 900 °C, and were connected in series to increase the measured voltage to ≈0.8 V. If one of the cells received significantly less light intensity than the other, then the first would act as a non-zero-ohm resistor. The light incident on the DM cells was assumed to be homogeneous by experimental design, therefore this effect was assumed to be negligible during the experiment.

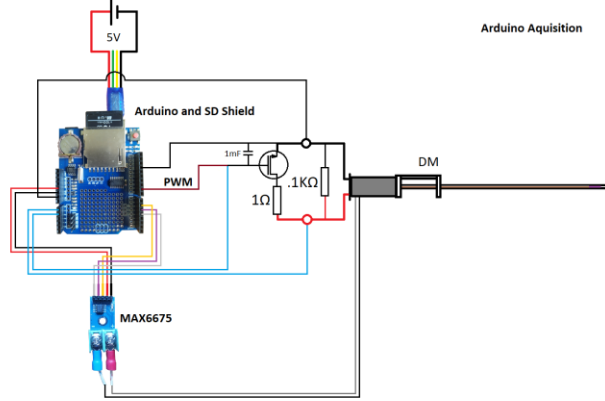


Fig 1: Setup illustration of the DM

A. Calibration

The calibration of the variable shunt was made with a bench top power supply. The power supply was set with a 1 V and 5A limit. The bench power supply was shorted across the variable shunt.

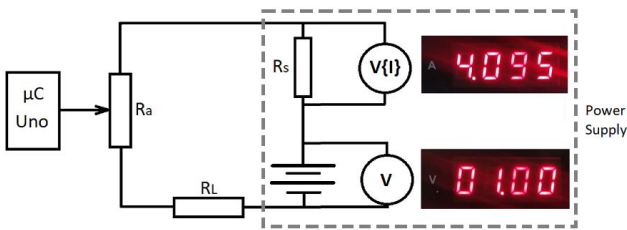


Fig 2: Illustration of calibration setup

Depending on the gate voltage of the transistor, R_a had a value of ≈100 Ω to →0 Ω. The ammeter and voltmeter measurements were correlated across the time of the sweep, see Fig 2 for an illustration of this setup.

A 14.8 Ω shunt resistor with a very stable value was shorted across the power supply. The voltage at the terminals was measured to be 1.006 V. The expected current in this scenario where the shunt is the only resistor would be 1.006 V/14.8 Ω = 0.06797 A. However, the in-built ammeter

displayed 0.065 A. The ammeter measurement used with the voltmeter measurement equate to a resistance of 1.006 V/0.065 A = 15.477 Ω. This new resistance value is the shunt of 14.8 Ω in addition to the line resistance (R_L) and the power supply’s ammeter shunt. Ergo, the resistance measured during the sweep can be shifted by a resistance of 15.477 Ω – 14.8 Ω = 0.677 Ω ± 0.322 Ω. The result, is a correlation of true resistance vs bit value of the PWM, see Fig 3.

This sweep data and its errors were loaded into a python script called “Calibration.py”. The script imports the scipy.optimize package to optimize the fit of some function to some data set. This function must be defined first, and the package optimizes the equation parameters to data using the R² method, see Fig 3.

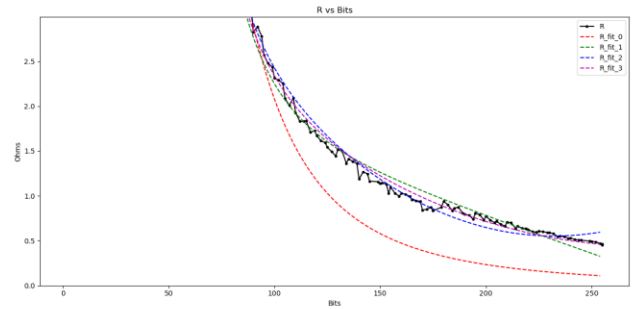


Fig 3: Zoomed graph showing different models to fit the trend of resistance as a dependent variable of bit value where R_fit_3 is the closest fit.

$$\Omega(\text{Bits}) = \frac{\left[\left(a \frac{1}{(b(\text{Bit})^c)^d} \right) + (e(\text{Bit}) + f) \right] + \left[\left(g \frac{1}{(h(\text{Bit})^i)^j} \right) + (k(\text{Bit})^2 + l(\text{Bit}) + m) \right]}{2} \quad (1)$$

Table 1: Calibration model parameters

a	b	c	d
0.61065423428	0.00183464929954	1.39625886387	4.1567876629
e	f	g	h
-0.0111315088	3.02102523421	0.47430105346	0.00890372331
i	j	k	l
1.0655781185	6.6203805599	0.00012734794	-0.0562351900
m	Bit		
6.7436944372	Var 0 to 255		

The parameters were used to re-plot the function. This was plotted with the original values and an R² value was calculated using equation 2. The R² value of “R_fit_3” was calculated to be 0.953. This fit was used to correlate bit of PWM to resistance of the variable shunt. The fit is shown in Fig 4. In Table 1 the parameters of this fit using (1) are shown.

$$R^2 = \frac{\sum \left((R_{data} - R_{prediction})^2 + (\Delta R_{data})^2 \right)}{\sum \left((R_{data} - \bar{R})^2 + (\Delta R_{data})^2 \right)} \quad (2)$$

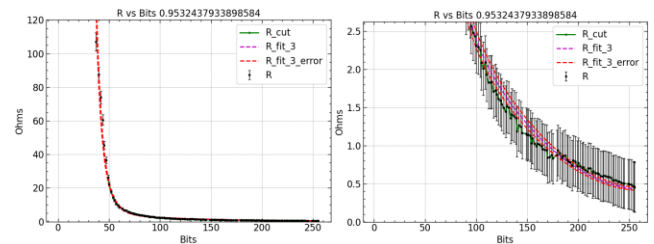


Fig 4: Calibration fit of a PWM sweep from bit 0 to bit 254 driving a variable resistor and optimized by SciPy

III. EXPERIMENTAL SETUP

A. Electric Furnace

An electric furnace was used first as it can reach the required temperatures homogeneously with little impact due to dust or corrosive gases. The electric oven was not used at temperatures greater than 900 °C to avoid damaging the glass. Multiple 20-minute acquisitions were taken at differing temperatures ranging from 500 °C to 900 °C. Another 900 °C run was taken for 2 hours and 35 minutes. This setup is shown in Fig 5.

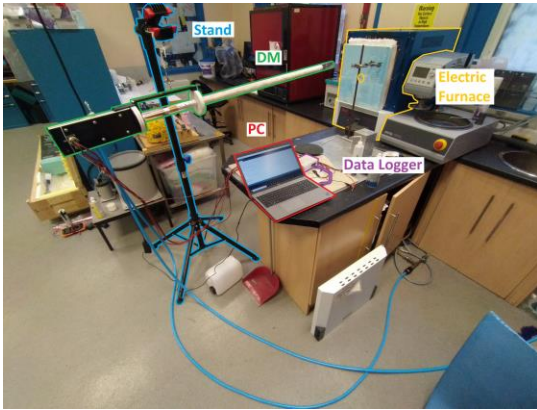


Fig 5: Electric oven setup with DM, data logging equipment and a retort stand

B. Cooldown Grate of A Cement factory

The DM was hoisted in place by Irish Cement staff using a port hole originally intended for instrument insertion as can be seen in Fig 6. Water flow was used at approximately 4 L/m and uninterrupted for the full duration of the experiment. Temperatures from tertiary instruments was reported to be at 1083 °C, which exceeds the 900 °C limit of the glass. The DM was therefore exposed to intervals for 1-minute durations which were repeated three times, allowing the glass to cool down between each acquisition sweep. This mitigated risk but limited the test duration.



Fig 6: Irish Cement cool down grate

IV. RESULTS

Testing took place in a TU Dublin laboratory and Irish Cement. These experiments were increasingly harsh as they progressed. The DM generated power for 2 hours 35 minutes at 900 °C.

Water was pumped in all experiments to ensure the TPV cell would remain cool. The furnace was brought up to a stable 900 °C before the DM was inserted. The output drift in voltage, current, and power was plotted. The oven temperature was lowered by 50 °C and allowed to settle. This was done incrementally until the ambient temperature in the oven was 500 °C. Below is a comparison between the voltage, current, and power of a typical sweep from 500 °C compared to 900 °C as shown in Fig 7. Approximately 22 sweeps each taking 51 seconds were taken for each temperature. The average of these was used to plot the power change with respect to environmental temperature. If Ambient light intensity could be measured, the efficiency of the TPV cells could be known. The light intensity and therefore the efficiency was estimated from calculation.

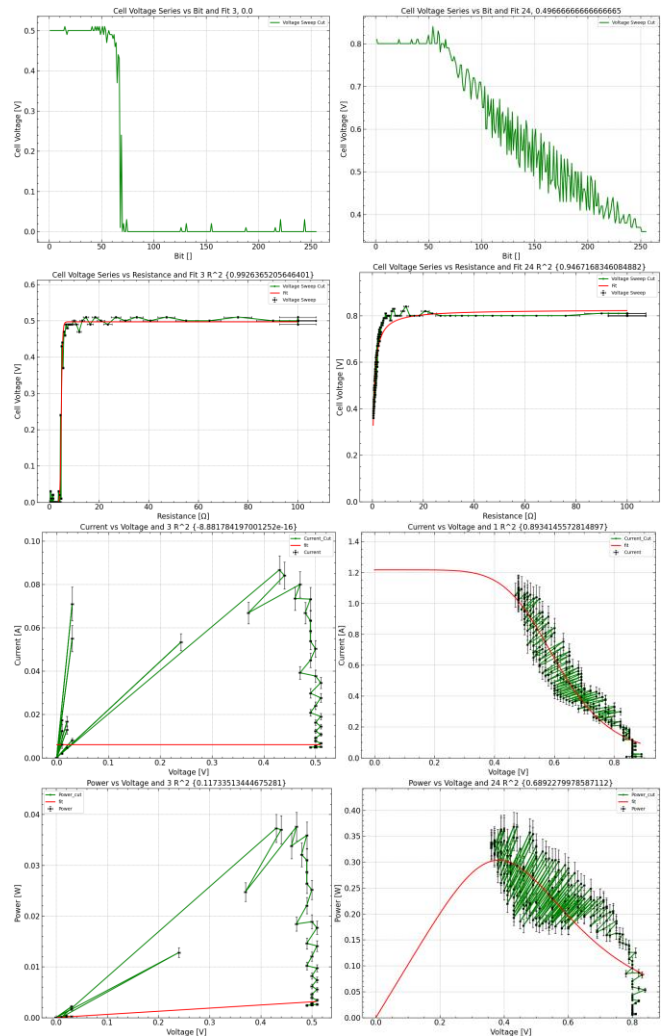


Fig 7: Left 500 °C acquisition compared to right 900 °C acquisition

The drift of the maximum voltage, current and power from the 500 °C and 900 °C measurement over 20 minutes is shown in Fig 8. These graphs show the maximum of a set of values and the maximum of a fitted model (shown in red in Fig 7). The voltage (V_{oc}) and current (I_{cc}) shown are not their optimal values needed to produce the maximum power. Power shown here is the MPP. Some data sweeps produced a data series too noisy to be automatically optimized within 1000 loops in software, particularly at low temperature and therefore low voltages. The maximum of the power data is

still shown in Fig 8 without the model values. The distribution of maximum current, voltage, and power was used to plot the change with respect to temperature.

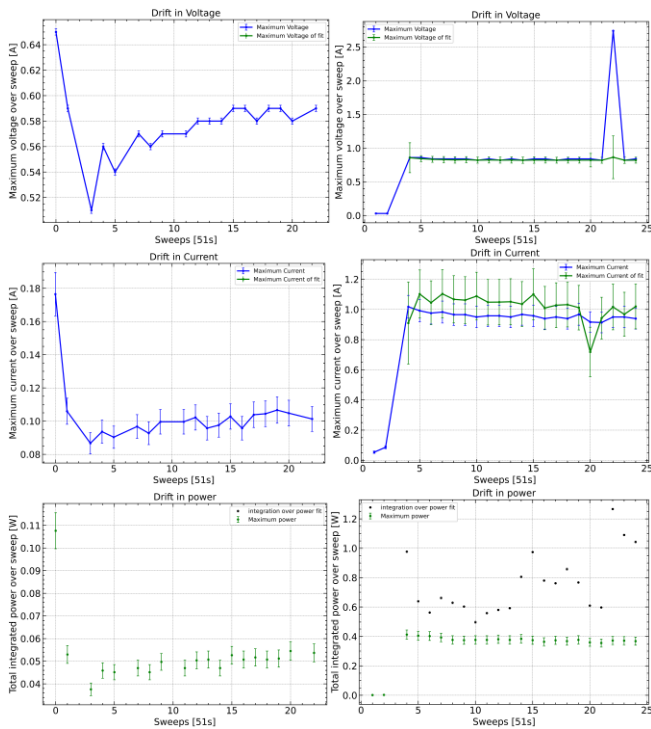


Fig 8: Left 500 °C acquisition compared to right 900 °C acquisition

The DM was also exposed to 900 °C for 2 hours 35 minutes, see Fig 9. The DM was unplugged to validate voltage reading with a multimeter during warmup.

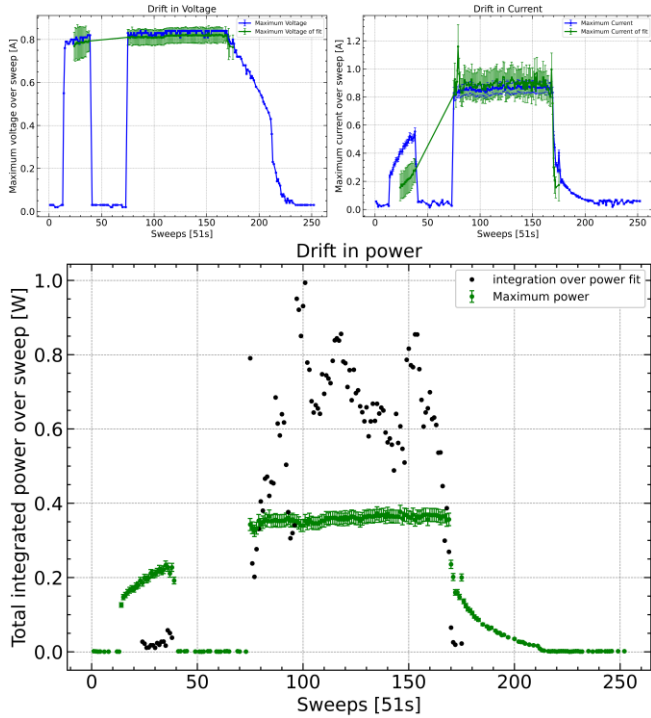


Fig 9: MPPT of DM exposed to electric furnace which reached a plateau of 900 °C

The MPP with respect to temperature of the DM is shown in Fig 10. The fit shown is a polynomial, which is not entirely

realistic. Theoretically, at a temperature of approximately 1400 °C, the power relation to temperature was expected to be optimized, after which the efficiency should start to decrease. A left-handed Gaussian curve is expected to represent the cells efficiency vs temperature. The mode of this Gaussian distribution is expected to occur at the band gap energy of the semiconductor. This is expected to coincide with Wien’s law at approximately 1400 °C.

The experimentation at Irish Cement produced less power than expected and took place after experiments in the electric furnace. This was due to the damage sustained at temperatures exceeding 950 °C. There was also a presence of dust and the shadowing of light incident of the cells that caused a higher internal resistance. Despite these problems the DM produced 0.16 W/cm². Three sweeps were taken at Irish Cement and the average MPP is shown in red, see Fig 10. This MPP was the model fit and not the maximum value. In chronological order the MPP was 0.172 W/cm², 0.163 W/cm², and 0.160 W/cm².

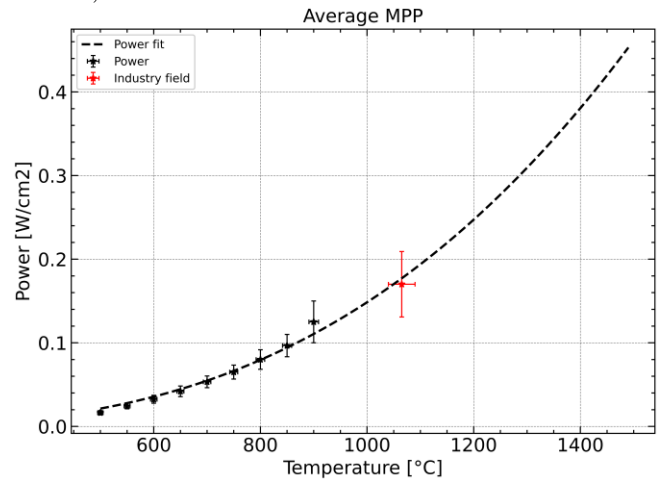


Fig 10: MPP of DM exposed to electric furnace and Irish Cement cool down grate.

A. Efficiency

Efficiency calculation requires the intensity of the incumbent light. Light energy falling on the TPV cell was calculated. The irradiance of the full spectrum produced by the heat source was calculated. The total wattage consumed by the oven is assumed to produce irradiated heat with 100% efficiency.

The input energy of the oven was supplied by electrical mains through a BS1363 domestic plug. Assuming a 13 A fuse was used in the oven the maximum continuous power draw was $(230\text{ V})(13\text{ A})(\cos(45)) \approx 2114\text{ W}$. A maximum power draw was assumed to be 2.1 kW. The elements are not continuously controlled (analogue) but were instead PWM. The elements were turned on until the desired temperature was measured by k-type thermocouple. The PWM was controlled by the oven to maintain the temperature. The average of the PWM power is the amount of heat loss of the oven. If the heat loss of the oven could be calculated, then the average PWM power could be presumed to compensate this loss. The elements heated up the surrounding material in the oven so the light flux on the TPV cells was smoothed. The cells did not see either 0 W or

2100 W but in fact the average PWM power to maintain a particular temperature.

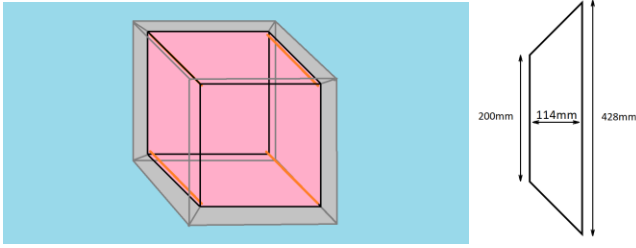


Fig 11: Heat loss from electric furnace with wall dimensions

(3) was used to calculate the heat loss at an instance of temperature. Where k is thermal conductivity, A is Area, L is thickness of the wall, T is temperature, Q describes rate of heat change in Watts.

$$\frac{dQ}{dt} = \dot{Q}[w] = kA \frac{T_1 - T_2}{L} \quad (3)$$

The volume inside the box was 0.2x0.2x0.2 m. The dimensions of the PROMATON®-23 HD, -26, -28 fire brick were 76 x 114 x 230 mm. The side thickness of the wall was 114 mm. Therefore, the outside must be 428 mm which was close to the measured height and width of the oven. The inside and outside of the wall were averaged and assume a wall length and breadth of 314mm see Fig 11. The thermal conductivity of the 26 grade AlSi Refractory Brick is variable dependent on temperature. Values from the AlSi-26 data sheet were used to create a model fit to them [12]. This model was included in (4).

The ambient temperature T_1 was assumed to be 293 °K and the insulation material to be grade-26 AlSi refractory brick. These assumptions were used to calculate the heat loss at all temperatures. A was 0.314x0.314 m, L was 0.114 m. The temperature inside the furnace was used to calculate the heat loss rate of Q dot. Convection was ignored as the total heat loss through all 6 walls was the same sum in any case.

$$\dot{Q} = \left((0.195e^{0.0004T_2})A \frac{T_1 - T_2}{L} \right) 6 \quad (4)$$

The heat loss through the refractory brick was calculated as a function of oven temperature. This can be used to calculate the intensity of all light under the Wien's displacement curve falling on the TPV cell. The elements are PWM, the refractory material is capacitive and emits stored energy in the form of light as well as conduct heat out of the system.

With an operating temperature of 900 °C and heat radiation surface of 0.24 m² the rate of heat change was 1428 W. ($Q \text{ dot} \times 1) / 2400 \text{ cm}^2 = 0.5950 \text{ W/cm}^2$ at the surface of the refractory material. The light intensity arriving at the TPV cell can be calculated by (5) where, I_d is the intensity at some distance, I is the source intensity, A is radiation area, and r is distance from the source. The average distance between cell and the walls was approximately 0.12 m. The incident light intensity on the cells at 900 °C was estimated to be 0.39 W/cm².

$$I_d = \frac{I}{A} = \frac{I}{4\pi r^2} \quad (5)$$

Table 2: Efficiency estimation calculation steps

Temp [°C]	E of Wein's peak [eV]	AlSi G26 Emissivity	Q' [W]	I at Cell [W/cm ²]	η
900	0.50	0.313	-1428	0.39	0.32
850	0.48	0.307	-1320	0.36	0.27
800	0.46	0.300	-1216	0.33	0.24
750	0.44	0.294	-1119	0.30	0.21
700	0.42	0.289	-1019	0.28	0.19
650	0.40	0.283	-925	0.25	0.16
600	0.38	0.277	-835	0.23	0.14
550	0.35	0.272	-748	0.20	0.12
500	0.33	0.266	-664	0.18	0.09

The efficiency was estimated for all power acquisitions of MPP. The actual intensity will be measured in future experiments. These efficiency estimates are shown in Table 2 and Fig 12. This efficiency estimation was compared to a maximum quantum efficiency calculation and experimental results for GaSb from previous relevant studies [11] [13]. A The optimal efficiency is assumed to take place where the Wien's displacement curve peak energy matches the band gap energy of the semiconducting material. The band gap energy of GaSb is 0.72 eV which is the same energy as the most intense part of the Wien's curve at an approximate temperature of 1400 °C. Therefore, the mode of the Gaussian was assumed to occur at 1400 °C. This will be experimentally validated in the future works.

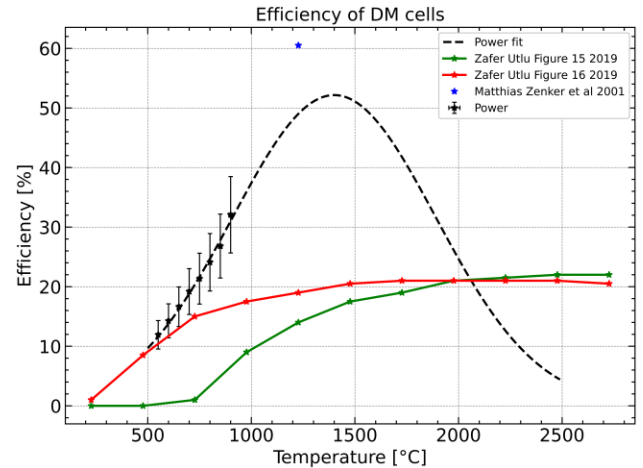


Fig 12: Efficiency estimate of DM exposed to electric furnace

V. CONCLUSION

The DM was a limited application of TPV technology that was sufficient for testing the concept. This enabled the automation of a system, also kept the cells at a safe distance between the heat source and the equipment. Known limits of the DM include:

- The cells area was very small 3cm²,

- The DM cells were on opposite sides of the heat exchanger,
- The quartz became opaque above 900 °C but the TPV cell is optimized at approximately 1400 °C.
- The line resistance was non-negligible because of long cables (12 m). The long cables were unshielded and act as antenna which created noise.
- There was a k-type thermocouple on the heat exchanger but no independent k-type thermocouple which would allow the DM to measure local temperature.

The setup of the existing DM can be improved. This mostly involves a more rigorous electrical setup. The DM was an electrical device and was heavily affected by sources of electrical noise. The MPP experiments produced good results, but without a measurement of the light intensity the efficiency was estimated from calculation.

A repeatability characterization was limited by the DM in design. A heat source must be acquired that can run continuously to obtain drift data. The DM suffered no noticeable damage due to the speed with which it was exposed to heat.

Testing with the DM predicted a power yield of approximately 4kW/m² using GaSb at 1400 °C at an estimated efficiency of approximately 50%. This prediction was based on testing with an electric furnace. Testing at Irish Cement exposed the DM to a harsh environment with unoptimized conditions for the DM. However, this provided a valuable industrial trial that highlighted further design considerations and proved the conception of the technology. At Irish Cement with an approximate temperature of 1065 °C, the DM produced 1.65 kW/m² at MPP. However, the DM was only operated for 3 minutes due to thermal limitations of the glass. The efficiency is predicted but must be validated by experiment.

VI. ACKNOWLEDGMENTS

This research was funded and supported through Enterprise Ireland under the project EI-CF2020-1381-P and was carried out with the help and support of TU Dublin and staff. The author would like to thank James Weir and the Irish Cement Staff for allowing the DM onsite providing helpful supervision and guidance with the testing at the cool down grate. The author would also like to thank Neil Branigan and Brendan Kennedy for the loan of their lab equipment and space as it was instrumental in gathering MPP and other critical data used to predict performance in more extreme environments.

VII. REFERENCES

- [1] Nelson, R.E., 2003. A brief history of thermophotovoltaic development. *Semiconductor Science and Technology*, 18(5), p.S141.
- [2] Hussain, C. M. I., Duffy, A. and Norton, B., 2020. Thermophotovoltaic systems for achieving high-solar-fraction hybrid solar-biomass power generation. *Applied Energy*, 259, p.114181.
- [3] Hussain, C. M. I., Norton, B., Duffy, A. and Oubaha, M., 2017. Hybrid Solar Thermophotovoltaic-Biomass/Gas Power Generation System with a Spectrally Matched Emitter for Lower Operating Temperatures.
- [4] Rashid, W.E.S.W.A., Ker, P.J., Jamaludin, M.Z.B., Gamel, M.M.A., Lee, H.J. and Abd Rahman, N.B., 2020. Recent development of thermophotovoltaic system for waste heat harvesting application and potential implementation in thermal power plant. *IEEE Access*, 8, pp.105156-105168.
- [5] Kolm H H 1956 "Solar-battery power source Quarterly, Progress Report", Solid State Research, Group 35, (Lexington, MA: MIT Lincoln Laboratory) p 13
- [6] Haushalter R W (1966), "Engineering investigation of a thermophotovoltaic energy converter Final Report", Contract No. DA-44-009-AMC-622(T) (Santa Barbara, CA: General Motors Defense Research Laboratories) p 185
- [7] Fraas, L., Ballantyne, R., Hui, S., Ye, S.Z., Gregory, S., Keyes, J., Avery, J., Lamson, D. and Daniels, B., 1999, March. Commercial GaSb cell and circuit development for the midnight sun® TPV stove. In *AIP Conference Proceedings* (Vol. 460, No. 1, pp. 480-487). American Institute of Physics.
- [8] Taizo Shibuya, Long History of Portable TPV Generator, CPV-18 & TPV-13 Conference 2022, Miyazaki Japan. (Si K.Kolm 1956, Ge Guazzoni 2004, GaSb Fraas 1999, GaSb Horne 2002, Si Durch 2008, InGaAs Chan 2017)
- [9] Chan, W.R., Stelmakh, V., Ghebrehbrhan, M., Soljačić, M., Joannopoulos, J.D. and Čelanović, I., 2017. Enabling efficient heat-to-electricity generation at the mesoscale. *Energy & Environmental Science*, 10(6), pp.1367-1371.
- [10] Chan, W.R., Stelmakh, V., Karnani, S., Waits, C.M., Soljagic, M., Joannopoulos, J.D. and Celanovic, I., 2018, July. Towards a portable mesoscale thermophotovoltaic generator. In *Journal of Physics: Conference Series* (Vol. 1052, No. 1, p. 012041). IOP Publishing.
- [11] Utlu, Z., 2020. Thermophotovoltaic applications in waste heat recovery systems: example of GaSb cell. *International Journal of Low-Carbon Technologies*, 15(2), pp.277-286.
- [12] PROMATON®-23 HD, -26, -28 Technical Data Sheet
- [13] Zenker, M., Heinzl, A., Stollwerck, G., Ferber, J. and Luther, J., 2001. Efficiency and power density potential of combustion-driven thermophotovoltaic systems using GaSb photovoltaic cells. *IEEE Transactions on Electron Devices*, 48(2), pp.367-376.